Editors' Suggestion

Pulsar Polarization Array Limits on Ultralight Axionlike Dark Matter

Xiao Xue,[1,2,3,*] Shi Dai,[4,*] Hoang Nhan Luu,[5] Tao Liu,[6,†] Jing Ren,[7,8,‡] Jing Shu,[9,8,10] Yue Zhao,[6] Andrew Zic,[4] N. D. Ramesh Bhat,[11] Zu-Cheng Chen,[12,13] Yi Feng,[14] George Hobbs,[4] Agastya Kapur,[4] Richard N. Manchester,[4] Rami Mandow,[15,4] Saurav Mishra,[16] Daniel J. Reardon,[16,17] Christopher J. Russell,[18] Ryan M. Shannon,[16,17] Shuangqiang Wang,[19,20] Lei Zhang,[21,16] Songbo Zhang,[22,4] and Xingjiang Zhu[23,24,25]

(PPTA Collaboration)

[1]*Institut de Física d'Altes Energies (IFAE), The Barcelona Institute of Science and Technology, Campus UAB, 08193 Bellaterra (Barcelona), Spain*
[2]*II. Institute of Theoretical Physics, Universität Hamburg, 22761 Hamburg, Germany*
[3]*Deutsches Elektronen-Synchrotron DESY, Notkestraße 85, 22607 Hamburg, Germany*
[4]*Australia Telescope National Facility, CSIRO Space and Astronomy, PO Box 76, Epping, NSW 1710, Australia*
[5]*Donostia International Physics Center, Basque Country UPV/EHU, San Sebastian, E-48080, Spain*
[6]*Department of Physics and Jockey Club Institute for Advanced Study, The Hong Kong University of Science and Technology, Hong Kong S.A.R., China*
[7]*Institute of High Energy Physics, Chinese Academy of Sciences, Beijing 100049, China*
[8]*Center for High Energy Physics, Peking University, Beijing 100871, China*
[9]*School of Physics and State Key Laboratory of Nuclear Physics and Technology, Peking University, Beijing 100871, China*
[10]*Beijing Laser Acceleration Innovation Center, Huairou, Beijing, 101400, China*
[11]*International Centre for Radio Astronomy Research, Curtin University, Bentley, West Australia 6102, Australia*
[12]*Department of Physics and Synergetic Innovation Center for Quantum Effects and Applications, Hunan Normal University, Changsha, Hunan 410081, China*
[13]*Institute of Interdisciplinary Studies, Hunan Normal University, Changsha, Hunan 410081, China*
[14]*Research Center for Astronomical Computing, Zhejiang Laboratory, 311121 Hangzhou, Zhejiang, China*
[15]*Department of Physics and Astronomy and MQ Research Centre in Astronomy, Astrophysics and Astrophotonics, Macquarie University, New South Wales 2109, Sydney, Australia*
[16]*Centre for Astrophysics and Supercomputing, Swinburne University of Technology, Hawthorn, Victoria, 3122, Australia*
[17]*ARC Centre of Excellence for Gravitational Wave Astronomy*
[18]*CSIRO Scientific Computing, Australian Technology Park, Locked Bag 9013, Alexandria, New South Wales 1435, Australia*
[19]*Xinjiang Astronomical Observatory, Chinese Academy of Sciences, Urumqi, Xinjiang 830011, China*
[20]*Australia Telescope National Facility, CSIRO, Space and Astronomy, PO Box 76, Epping, NSW 1710, Australia*
[21]*National Astronomical Observatories, Chinese Academy of Sciences, A20 Datun Road, Chaoyang District, Beijing 100101, China*
[22]*Purple Mountain Observatory, Chinese Academy of Sciences, Nanjing 210023, China*
[23]*Department of Physics, Faculty of Arts and Sciences, Beijing Normal University, Zhuhai 519087, China*
[24]*Institute for Frontier in Astronomy and Astrophysics, Beijing Normal University, Beijing 102206, China*
[25]*Advanced Institute of Natural Sciences, Beijing Normal University, Zhuhai 519087, China*

(Received 24 July 2024; revised 22 September 2025; accepted 9 December 2025; published 7 January 2026)

We conduct the first-ever pulsar polarization array (PPA) analysis to detect the ultralight axionlike dark matter (ALDM) using the polarization data of 22 millisecond pulsars from the third data release of Parkes pulsar timing array. As one of the major dark matter candidates, the ultralight ALDM exhibits a pronounced wave nature on astronomical scales and offers a promising solution to small-scale structure issues within local galaxies. While the linearly polarized pulsar light travels through the ALDM galactic halo, its position angle (PA) can be subject to an oscillation induced by the ALDM Chern-Simons coupling with electromagnetic field. The PPA is thus especially suited for detecting the ultralight ALDM by correlating polarization data across the arrayed pulsars. To accomplish this task, we develop an advanced Bayesian analysis framework that allows us to construct pulsar PA residual time series, model noise contributions properly and search for pulsar cross-correlations. We find that for an ALDM density of $\rho_0 = 0.4$ GeV/cm^3,

*These authors contributed equally to this work.
†Contact author: taoliu@ust.hk
‡Contact author: renjing@ihep.ac.cn

the Parkes PPA offers the best global limits on the ALDM Chern-Simons coupling, namely $\lesssim 10^{-13.5} - 10^{-12.2}$ GeV^{-1}, for the mass range of 10^{-22}–10^{-21} eV. The crucial role of pulsar cross-correlation in recognizing the nature of the derived limits is also highlighted.

DOI: 10.1103/mptv-3x6g

Introduction—Millisecond pulsars (MSPs) are known as astronomical clocks due to the remarkable regularity of their pulses. The Pulsar timing array (PTA), consisting of many accurately timed MSPs in the Milky Way, thus has been proposed as a galactic-scale detector for nanohertz gravitational waves (GWs) [1,2]. The Hellings-Downs (H-D) curve [3] plays a crucial role in recognizing the signals of stochastic GW background (SGWB), as it manifests the unique correlation of signal-induced timing residuals across the MSPs. Recently, four leading PTA collaborations [4–7] reported a consistency between their data and the H-D curve, strongly supporting the SGWB interpretation of the observed common process excess. This milestone for GW astronomy marks a roaring success for the PTA programs.

Pulsars are also known as excellent astronomical linear polarization sources. Their light can be linearly polarized to wellabove 10% of total intensity. The PTA programs usually measure the pulsar polarization profiles for calibrating the relevant observations [8]. Vast amounts of polarization data thus exist or are expected to be collected in the active PTAs and other pulsar-monitoring programs. This has motivated the suggestion of developing pulsar polarization arrays (PPAs) [9], to explore astrophysics and fundamental physics with a correlated polarization signal across the pulsars. One representative scientific case is detecting ultralight axionlike dark matter (ALDM).

Dark matter (DM) makes up ∼85% of the matter in the universe, yet its nature remains uncertain. The ALDM is one of the major theories to explain the DM observations. The concept of an axion arose originally to address the strong charge-parity problem in quantum chromodynamics, while many particle physics theories predict axion-like particles. The ultralight ALDM, due to its long de Broglie wavelength, is distinguished from the other DM candidates by its wave nature at astronomical scales. Of particular interest is the ultralight ALDM with a mass of 10^{-22}–10^{-21} eV, generally known as "fuzzy DM" [10,11], which offers a potential solution to the "small-scale" structure problems [10–12]. The constraints on this DM scenario may arise from the observations of Lyman-α forest and dwarf galaxies (for a review, see Ref. [13]). As these constraints are under debate [13–16], it is highly valuable to develop independent probes.

The PPA is especially suited for the detection of the ultralight ALDM. Due to condensation, the ALDM galactic halo can be described as a classical field [17]. The ALDM field couples to an electromagnetic (EM) field via the Chern-Simons term $\sim \frac{1}{2} g_{a\gamma\gamma} a F_{\mu\nu} \tilde{F}^{\mu\nu}$. Here a is the ALDM field, $F_{\mu\nu}$ is the EM field strength and $\tilde{F}_{\mu\nu}$ is its Hodge dual, and $g_{a\gamma\gamma}$ is the Chern-Simons coupling. The ALDM halo as a background breaks the degeneracy of dispersion relation between the left- and right-circular polarization modes of light because of its odd parity. As a result, while the linearly polarized pulsar light travels through the ALDM halo, its position angle (PA) can rotate. This effect in a general context is known as "cosmic birefringence (CB)" [18,19]. The ALDM wave nature at astronomical scales predicts a signature of oscillating PA with specific pattern in space-time [9]. The PPA by cross-correlating the data is thus expected to be highly capable of recognizing the ultralight ALDM signals.

In this letter, we conduct the first-ever PPA analysis to search for the ultralight ALDM, using the polarization data of 22 MSPs from PPTA Data Release 3 (DR3) [6,20]. We denote this PPA as the Parkes PPA (PPPA) for the convenience of discussions. To accomplish this task, we develop an advanced analysis framework tailored specifically for constructing real pulsar PA residual time series, modeling instrumental and astronomical noises, and searching for signal correlation across the arrayed pulsars. Using this Bayesian framework, we demonstrate that the PPPA provides the most stringent constraints on the ALDM Chern-Simons coupling within the relevant mass range. Notably, we demonstrate for the first time that the pulsar cross-correlation plays a crucial role in investigating the nature of the derived limits.

ALDM induced cosmic birefringence—The DM halos originate from primordial density fluctuations, with the DM particles becoming virialized over the galaxy history [21]. Consequently, the ultralight ALDM field can be viewed as a random superposition of a vast number of plane waves [22–25]:

$$a(\mathbf{x},t) \approx \frac{\sqrt{\rho(\mathbf{x})}}{m_a} \sum_{\mathbf{v}\in\Omega} (\Delta v)^{3/2} \alpha_{\mathbf{v}} \sqrt{f_{\mathbf{x}}(\mathbf{v})} \times \cos[m_a(t - \mathbf{v}\cdot\mathbf{x}) + \phi_{\mathbf{v}}], \quad (1)$$

where $\rho(\mathbf{x})$ is ALDM energy density at position $\mathbf{x}$, m_a is ALDM mass, $\mathbf{v}$ denotes velocity in a latticed phase space Ω, and Δv is lattice spacing. $f_{\mathbf{x}}(\mathbf{v})$ represents DM velocity distribution at $\mathbf{x}$, which is assumed to be spatially uniform and isotropic, with the speed $|\mathbf{v}|$ peaking at the halo's virial velocity, i.e., $v_0 \sim \mathcal{O}(100)$ km/s. The profile of $\rho(\mathbf{x})$ is determined by Schrödinger-Poisson equations. As shown

in [26], the halo self-gravitation leads to the formation of a central solitonic core within galaxies. Since most PPPA MSPs are only $\lesssim\mathcal{O}(10^3)$ parsec away from the Earth, we simply assume $\rho(\mathbf{x})$ to be uniform, i.e., $\rho(\mathbf{x})=\rho_0$ [27], with its value to be determined by galactic halo measurements. The parameters $\alpha_{\mathbf{v}}\in(0,+\infty)$ and $\phi_{\mathbf{v}}\in(0,2\pi)$ represent random amplitude and phase, respectively, following Rayleigh and uniform distributions [22]. For a specific realization of $\{\alpha_{\mathbf{v}},\phi_{\mathbf{v}}\}$, the ALDM field $a(\mathbf{x},t)$ exhibits stochastic spacetime dependence [23], where coherence gets lost for a temporal interval $\gg\tau_c$ or a spatial interval $\gg l_c$, with $\tau_c\sim 1/(m_a v_0^2)$ and $l_c\sim 1/(m_a v_0)$ denoting the coherent time and coherent length (i.e., de Broglie wavelength) of this field. For the mass range of ultralight ALDM, the observation period $T_{\rm obs}$ for existing PTA programs is significantly shorter than τ_c, leading to coherent temporal evolution of $\cos(m_a t+\ldots)$ within this period as shown in Eq. (1). However, the distances of pulsars, whether to another pulsar or to the Earth, may exceed l_c, resulting in stochastic variation of the ALDM field over such distances.

Given the ALDM field within the Milky Way, one can calculate the induced PA residual $\Delta\mathrm{PA}^a$ for the linearly polarized pulsar light. As the CB effect is topological [28], $\Delta\mathrm{PA}^a$ depends on the $a(\mathbf{x},t)$ values solely at two endpoints of the light path. For a pulse emitted at $(\mathbf{x}_p,t_p)$ from the pulsar and received at $(\mathbf{x}_e,t_e)$ on the Earth, we have

$$\Delta\mathrm{PA}^a\approx g_{a\gamma\gamma}[a(\mathbf{x}_p,t_p)-a(\mathbf{x}_e,t_e)], \tag{2}$$

where the two terms are dubbed "pulsar" and "Earth" terms. The $\Delta\mathrm{PA}^a$ magnitude can be characterized by a parameter $S_a\equiv g_{a\gamma\gamma}\sqrt{\rho_0}/m_a$ then. For $m_a\sim 10^{-22}$ eV and $\rho_0\sim 0.1$ GeV/cm^3, this implies that a signal of $\Delta\mathrm{PA}^a\sim 0.1$ deg needs the Chern-Simons coupling to be $g_{a\gamma\gamma}\sim 10^{-13}$ GeV^{-1}. Note, while the SGWB-induced timing residual in the PTA is also determined by so-called "pulsar" and "Earth" terms, unlike the CB effect, it arises from a cancellation between contraction and expansion of the light path as the GWs pass by. Moreover, the CB is distinguished from the Faraday rotation in interstellar medium (ISM) and Earth's ionosphere as the latter effect is frequency dependent and relies on the length of light path aligned with the direction of magnetic field.

PPA analysis framework—In last decade, a few attempts have been made to explore temporal variations of pulsar polarization [29–31]. The PA residuals of individual pulsars have been suggested for testing the ALDM theory [32,33]. However, a systematic analysis framework of the PPA, which emphasizes the data correlation across the pulsars, remains absent. To address this, we model the PA residuals as

$$\Delta\mathrm{PA}^{\rm obs}=\Delta\mathrm{PA}^a+\Delta\mathrm{PA}^{\rm ion}+\Delta\mathrm{PA}^w+\Delta\mathrm{PA}^r+\Delta\mathrm{PA}^{\rm pol}. \tag{3}$$

Besides the stochastic signal $\Delta\mathrm{PA}^a$ defined in Eq. (2), there are additional components categorized as deterministic and random. The deterministic components include the Faraday rotation induced by the Earth's ionosphere, $\Delta\mathrm{PA}^{\rm ion}$, which varies over timescales from hours to years and is derived with the package ionFR. The random contributions consist of white noise, $\Delta\mathrm{PA}^w$, which incorporates radiometer noise and accounts for random pulse-to-pulse variations in polarization profiles, along with unmodeled ionospheric effects that persist after the ionFR subtraction on shorter timescales. Red noise, $\Delta\mathrm{PA}^r$, is also random and captures variations in ISM Faraday rotation or fluctuations in dispersion measure and rotation measure and unmodeled ionospheric effects over years using a frequency-domain power spectrum. Additionally, we model long-term effects observed in the data with a polynomial of up to second order, denoted by $\Delta\mathrm{PA}^{\rm pol}$, which may account for slow stochastic changes in ISM properties over decades [see Supplemental Material (SM) at Sec. B for details [34]].

The ALDM signal nature can be encoded in its covariance matrix $\boldsymbol{C}^a$, as a two-point correlation function of $\Delta\mathrm{PA}^a$ [9]. In the data, $\Delta\mathrm{PA}^a$ is constructed as a vector $\{\Delta\mathrm{PA}^a_{p,n}\}$, where p runs over all PPA pulsars and n runs over all epochs for each of them. Inheriting from the ALDM properties [24], this vector follows a multivariate Gaussian distribution with zero mean. By integrating the velocity of ALDM particles with a delta-function approximation for the speed at $|\mathbf{v}|=v_0$, we find $C^a_{p,n;q,m}\approx S_a^2\hat{C}^a_{p,n;q,m}$ [9], where

$$\begin{aligned}\hat{C}^a_{p,n;q,m}=&\cos[m_a(t_{p,n}-t_{q,m})]\\&+\cos[m_a(t'_{p,n}-t'_{q,m})]\mathrm{sinc}(y_{pq})\\&-\cos[m_a(t'_{p,n}-t_{q,m})]\mathrm{sinc}(y_{ep})\\&-\cos[m_a(t_{p,n}-t'_{q,m})]\mathrm{sinc}(y_{eq})\end{aligned} \tag{4}$$

reflects quadratic interplay of its Earth and pulsar terms [see Eq. (2)]. $\hat{C}^a_{p,n;q,m}$ is essentially a correlation measure. In its expression, $t_{p,n}$ and $t'_{p,n}=t_{p,n}-D_p$ denote the light reception and emission time for the nth epoch of the pth pulsar, with D_p being the pulsar distance to the Earth, and their cosine functions denote temporal correlations of pulsar signals. The sinc functions $\mathrm{sinc}(y_{ij})\equiv\sin(y_{ij})/y_{ij}$ are all related to the pulsar term and manifest signal spatial correlations. Here, $y_{ij}\equiv|\mathbf{x}_i-\mathbf{x}_j|/l_c$ is a dimensionless distance parameter. These spatial correlations get suppressed when $|\mathbf{x}_i-\mathbf{x}_j|$ is significantly greater than the coherence length l_c.

These correlations originate from the spacetime dependence of the ALDM field phase factor [see Eq. (1)] or equivalently the ALDM wave nature. All terms in $\hat{C}^a_{p,n;q,m}$ can contribute significantly to recognizing the ALDM signals [9]. Due to its nonrelativistic nature, the ALDM

de Broglie wavelength is approximately three orders of magnitude longer than its Compton wavelength ($\sim 1/m_a$). The nanoHz ($\sim 10^{-23.4}$ eV) ALDM thus has a de Broglie wavelength $\sim$1.5 kpc, yielding $y_{ij} \lesssim 1$ for many PPPA pulsars. This outcome contrasts with the PTA response to the nanoHz SGWB, where the H-D curve arises from the interplay between the Earth terms, and the pulsar terms are less important since the de Broglie wavelength of GWs is simply their Compton wavelength and hence much shorter than general pulsar distances for the current PTAs.

For the PPA analysis, the matrix $\boldsymbol{C}^a$ defines a signal model with full correlation, with its diagonal ($p = q$) and off-diagonal blocks ($p \neq q$) manifesting the pulsar auto-correlation and cross-correlation, respectively. Below, we will focus on the full-correlation signal model, and as a reference, consider also the autocorrelation-only model where $\hat{C}^{a,\mathrm{auto}}_{p,n;q,m} = \hat{C}^{a}_{p,n;q,m}\delta_{pq}$.

The sensitivity analysis is based on Bayesian statistics. It is performed using the likelihood function [9]

$$\ln \mathcal{L} = -\frac{1}{2}\widetilde{\Delta \mathrm{PA}}^T \boldsymbol{C}^{-1} \widetilde{\Delta \mathrm{PA}} - \frac{1}{2}\ln |2\pi \boldsymbol{C}|. \tag{5}$$

Here $\widetilde{\Delta \mathrm{PA}} \equiv \Delta \mathrm{PA}^{\mathrm{obs}} - \Delta \mathrm{PA}^{\mathrm{ion}} - \Delta \mathrm{PA}^{\mathrm{pol}}$ is the time series of PA residuals with $\Delta \mathrm{PA}^{\mathrm{ion}}$ and $\Delta \mathrm{PA}^{\mathrm{pol}}$ subtracted. $\boldsymbol{C} = C^w + C^r + S_a^2 \hat{C}^a$ is the full covariance matrix that includes the contributions of the white and red noises and the ALDM signals. For the parameter S_a, we set the average ALDM energy density $\rho_0 = 0.4\ \mathrm{GeV/cm^3}$ [79] as the benchmark, since the Milky Way inner region ($\sim$20 kpc), where its rotation curve is measured for determining the local DM density [80] is considerably larger than l_c for the mass range considered below. Then by integrating out the $\Delta \mathrm{PA}^{\mathrm{pol}}$ parameters we obtain a likelihood parameterized by $\{\theta_n, D_p^*, m_a, S_a\}$, where θ_n denotes the set of random noise parameters, and D_p^* is a pulsar distance normalized by the measured central value. To determine the spatial correlations in Eq. (4), we account for the D_p^* uncertainties using priors determined by the measurement methods. For any given ALDM mass, we then perform a Bayesian analysis to constrain S_a with this marginalized likelihood. Eventually, we convert the posterior distributions of S_a to the limits on the ALDM Chern-Simons coupling for the given benchmark value of ρ_0. In addition to imposing limits, we use two Bayes factors $\mathrm{BF}^{\mathrm{Full}}_{\mathrm{Null}}$ and $\mathrm{BF}^{\mathrm{Full}}_{\mathrm{Auto}}$ to compare the full-correlation signal model with the null-signal model and to differentiate it from the autocorrelation-only signal model, respectively. The latter is particularly crucial for understanding the nature of the derived limits and recognizing the real signals in the data (see SM at Secs. A and B for details [34]).

PPA results and discussions—The PPTA DR3 [20] includes the measurements of Stokes parameters for 32 MSPs in the radio band, with a period from 2004 to 2022. We reprocess all data taken with the Ultra-Wideband Low receiver system, with the most up-to-date polarization calibration model to improve the measurement quality [81], and correct for static Faraday rotations caused by the ISM using the rotation measures provided by the Australia Telescope National Facility pulsar catalog [82]. We then select 22 MSPs for the PPPA construction whose signal-to-noise ratio of linear polarization intensity is relatively high in the considered frequency band (2.6–3.6 GHz). For these MSPs, we align the observation in each epoch with the PPTA template of total intensity [20,83]. We then derive the standard PA profiles, subtract them from the data, and perform a weighted average over the phase bins, to generate PA residual time series for unbiased signal estimation (see SM at Sec. A for details [34]).

We then test the noise model for individual MSPs using the likelihood in Eq. (5), with the ALDM signal turned off. To achieve this, we introduce a set of Bayes factors as a metric to assess the improvements in noise modeling by adding additional noise components one at a time to the minimal noise model, ultimately leading to the full noise model (see Table II at Sec. B of SM for details [34]). Compared to the minimal model including only the observation error of $\Delta \mathrm{PA}^{\mathrm{obs}}$ and a constant residual [9], the full noise model shows a remarkable improvement in fitting the data for the majority of the 22 PPPA MSPs. The most significant improvements are observed for J0437-4715, J1713 + 0747 and J1909-3744. The contribution of each new component vary greatly among different pulsars. The analysis suggests that the imperfect modeling of ionospheric Faraday rotation may account for the additional white noise and even red noise observed for some specific pulsars, while slow change of the ISM properties over decades could explain the observed long-term linear and quadratic variations. This outcome fully demonstrates the effectiveness of incorporating new noise components in modeling the observed PA residuals in Eq. (3).

We demonstrate in Fig. 1 the 95% upper limits on the ALDM characteristic signal strength S_a as a function of m_a, for six representative PPPA MSPs individually. For the mass range of $m_a \gtrsim 1/T_{\mathrm{obs}}$, the S_a limits are relatively flat. A best limit as strong as 0.1 deg or even stronger can be achieved for many of these pulsars including J0437-4715, J1744-1134, J1022 + 1001, etc. As the ALDM mass decreases to below $1/T_{\mathrm{obs}}$, the limits deteriorate approximately with m_a^{-3}, consistent with the expectation from integrating $\Delta \mathrm{PA}^{\mathrm{pol}}$ as a second-order polynomial expansion [84]. The ionospheric subtraction effectively removes sharp peaks around $\sim$1 yr or/and low-frequency excess for J0437-4715, J1600-3053 and J1744-1134. The incorporation of additional white noise component enhances the limits for six pulsars uniformly, and of red noise component improves intermediate- and low-frequency limits for J0437-4715 and J1909-3744 notably. These analyses show that, due to the variance of noise nature over pulsars, the

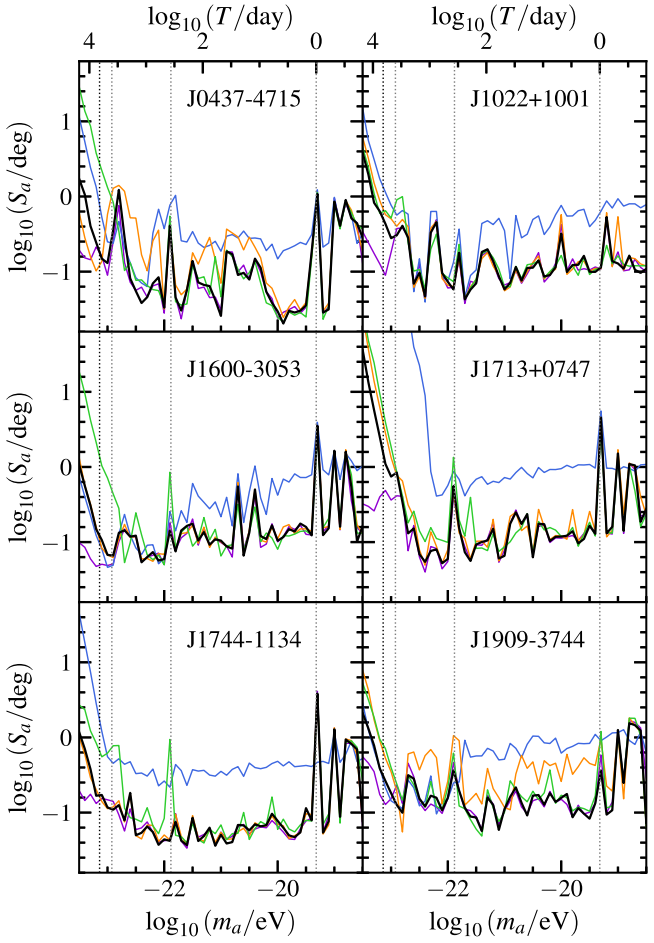

FIG. 1. 95% upper limits on the ALDM characteristic signal strength S_a as a function of its mass m_a, for six representative PPPA MSPs. In each panel, the black solid line represents the single-pulsar limits with full noise modeling in Eq. (3), while the colored lines show the limits excluding individual noise components: additional white noise (blue), red noise (orange), linear and quadratic long-term noise (purple), and ionospheric effects (green). The difference between the black and colored lines reflects the contribution of each noise component to the analysis. As a reference, we present $T_{\rm obs}$ of each pulsar, and timescales of solar cycle (11 years), one year, and one day, as colored and gray vertical dotted lines, respectively. The timescale and m_a are related by $m_a = 2\pi/T$.

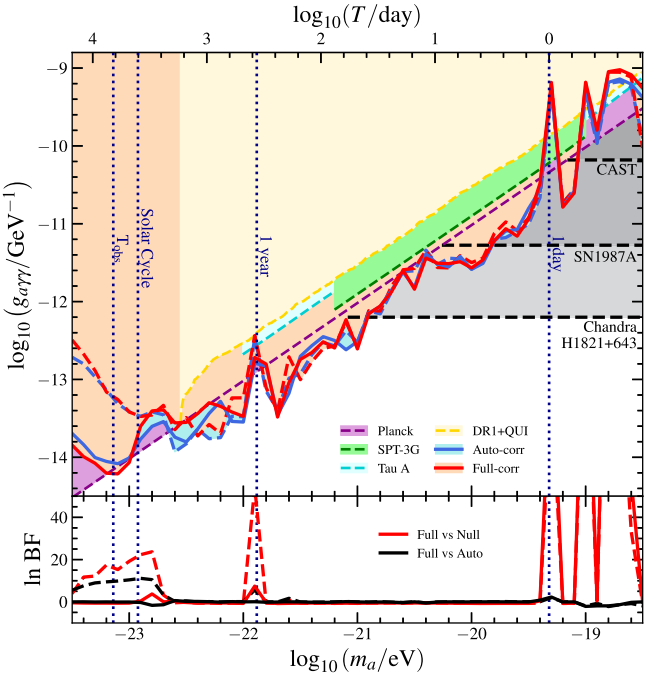

FIG. 2. 95% upper limits of the PPPA on the ALDM Chern-Simons coupling $g_{a\gamma\gamma}$ as a function of its mass m_a, with $\rho_0 = 0.4$ GeV/cm^3. The blue and red curves represent the limits obtained with the autocorrelation-only and full-correlation signal models, respectively, with (solid) and without (dashed) the ionospheric subtraction. As a reference, the smoothened constraints from the observation of PA variation in Crab Nebula with POLARBEAR [85], the analysis of PPTA data of DR1 and Crab Nebula data from QUIJOTE [86], the measurement of the CMB polarization with SPT-3G [87], and the investigation of PLANCK mission on the ALDM-induced washout effects during recombination [88] are presented as cyan, yellow, green, and purple dashed lines. The limits from the CAST experiment [89] and the observations of SN1987A [90] and x-ray spectral distortion in quasar H1821 + 643 [91] are also presented as black dashed lines. The shaded regions above these lines indicate the range of m_a and $g_{a\gamma\gamma}$ that they have excluded. The vertical dotted lines denote the reference timescales, including the PPPA observation period $T_{\rm obs} \approx 18$ yrs, solar cycle, one year, and one day. In the lower subpanel, the Bayes factors are displayed in two scenarios: the full-correlation signal model against the null-signal model (red) and the full-correlation signal model against the autocorrelation-only signal model (black).

advanced noise model in Eq. (3) is essential for getting robust limits on the ALDM signal strength (see SM at Sec. B for details [34]).

The final PPPA limits on the ALDM Chern-Simons coupling $g_{a\gamma\gamma}$ are presented in Fig. 2 as a function of its mass m_a, for both full-correlation and autocorrelation-only signal models. These limits exhibit a linear dependence on m_a for $m_a \gtrsim 1/T_{\rm obs}$, while scale as m_a^{-2} for $m_a \lesssim 1/T_{\rm obs}$. This feature should be expected from the scaling behavior of the S_a limits depicted in Fig. 1. Moreover, one can see that the ionospheric subtraction softens the peak at the timescale of 1 year in these limits. These limits, however, start to oscillate strongly as the timescale decreases to one day or shorter, resulting in some sharp peaks for $m_a \gtrsim 10^{-19.4}$ eV.

To recognize the nature of these derived limits, we also present two Bayes factors in this figure. The overall uniformity of $\ln {\rm BF}^{\rm Full}_{\rm Auto} \sim 0$ for the considered mass range implies that no significant ALDM signals have been detected in the PPPA data. Particularly, despite the peaks of $\ln {\rm BF}^{\rm Full}_{\rm Null}$ at the timescales of one day or shorter, the approximate flatness in the $\ln {\rm BF}^{\rm Full}_{\rm Auto}$ curve indicates a deficiency in the data of the ALDM-induced cross

correlation. These sharp peaks in the limits are thus more likely to be caused by imperfect noise modeling. This discussion can be applied to the peak observed for the limits at $m_a \sim 10^{-22}$ eV also. It highlights the crucial role played by the cross correlation in recognizing the nature of the data.

In Fig. 2, we also present two categories of additional limits as a reference. The first category does not rely on the ALDM assumption, including the limits from CAST [89], SN1987A [90] and H1821 + 643 [91]. Since the signals arise from relativistic axionlike particles, the generated limits are flat up to the energy scale of their production. The second category is to search for the ALDM-induced oscillations in polarization data, including the analyses of PPTA-QUIJOTE [86], CMB [87], and Crab Nebula [85]. The method in Ref. [88] is based on washout effects caused by ALDM-induced oscillations on the CMB during the recombination era, which benefits from the relatively high DM density in the early universe. As these studies are ALDM-based, the derived limits on $g_{a\gamma\gamma}$ exhibit similar scaling features with m_a to that of the PPPA limits. The PPPA provides the most stringent limits across a wide mass range within this category, and varying the value of ρ_0 does not change their relative positions. For a local density value of $\rho_0 = 0.4$ GeV/cm^3, especially, the PPPA offers the best global limits, namely $\lesssim 10^{-13.5} - 10^{-12.2}$ GeV^{-1}, for the mass range of fuzzy DM of 10^{-22}–10^{-21} eV. Thanks to the 18-year observation time span of PPTA DR3, its excellent sensitivities extend to $\sim 10^{-23}$ eV.

Conclusion and outlook—In this Letter, we presented the first-ever PPA analysis to detect the ultralight ALDM, using the polarization data from the PPTA DR3. We developed a systematic analysis framework for this task, including proper data construction, advanced noise modeling, and robust Bayesian sensitivity analysis. The derived limits are found to be superior to the existing ones for the mass range of fuzzy DM and hence represents the globally best. Particularly, the data correlation across the pulsars plays a pivotal role in recognizing the nature of these limits. This Letter represents an initial effort to investigate the great physical potential of current and forthcoming polarization data of pulsars. Besides further improvements of the developed PPA analysis framework, especially its noise modeling, several significant scientific tasks can be readily recognized for future explorations.

First of all, we can further advance the PPA applications for the ALDM detection. The PPA as an innovative tool is universal and can be built up with polarization data from other PTA programs also and even with broad datasets of normal pulsars. Moreover, we can synergize the PPA and the PTA. The ALDM halo can periodically perturb the spacetime metric and hence be detected by the PTA [92–96], especially through pulsar cross-correlation [99]. By constructing a PPA-PTA detector where the polarization and timing signals are correlated, the capability of a pulsar array could be further enhanced [97]. Finally, the current PTA and PPA analyses could be extended from the radio band to high frequencies. With the pulsar data collected by Fermi Large Area Telescope, the first γ-ray PTA constraints on the SGWB have been delivered in [98] and on the ultralight ALDM in [99,100]. We would expect the current and forthcoming x-ray missions, such as the Imaging X-ray Polarimetry Explorer [101] and the Enhanced X-ray Timing and Polarimetry [102], to offer valuable insights on this task for the PPA. We leave these explorations to future work.

Acknowledgments—X. X. is supported by Deutsche Forschungsgemeinschaft under Germany's Excellence Strategy EXC2121 "Quantum Universe" (390833306). The IFAE is partially funded by the CERCA program of the Generalitat de Catalunya. X. X. was partly funded by Grants No. CNS2023-143767 and No. CNS2023-143767 funded by MICIU/AEI/10.13039/501100011033 and by the European Union NextGenerationEU/PRTR. T. L. is supported by the Collaborative Research Fund under Grant No. C6017-20G, which is issued by the Research Grants Council of Hong Kong SAR. J. R. is supported in part by the National Natural Science Foundation of China under Grant No. 12435005. J. S. is supported by Peking University under startup Grant No. 7101302974 and the National Natural Science Foundation of China under Grants No. 12025507 and No. 12150015; and is supported by the Key Research Program of Frontier Science of the Chinese Academy of Sciences (CAS) under Grant No. ZDBS-LY-7003. Y. Z. is supported by U.S. Department of Energy under Award No. DESC0009959. Z. C. C. is supported by the National Natural Science Foundation of China (Grants No. 12247176 and No. 12247112) and the innovative research group of Hunan Province under Grant No. 2024JJ1006. Parts of this work were undertaken with the support of the Australian Research Council Centre of Excellence for Gravitational Wave Discovery (CE230100016). L. Z. is supported by a ACAMAR Postdoctoral Fellowship and the National Natural Science Foundation of China (Grant No. 12103069). X. J. Z. is supported by the National Natural Science Foundation of China (Grant No. 12203004) and by the Fundamental Research Funds for the Central Universities.

Data availability—The data that support the findings of this article are openly available [103].

[1] S. Detweiler, Astrophys. J. **234**, 1100 (1979).
[2] R. S. Foster III, *Constructing a Pulsar Timing Array* (University of California, Berkeley, 1990).
[3] R. Hellings and G. Downs, Astrophys. J. **265**, L39 (1983).
[4] G. Agazie *et al.* (NANOGrav Collaboration), Astrophys. J. Lett. **951**, L8 (2023).

[5] J. Antoniadis *et al.* (EPTA and InPTA Collaborations), Astron. Astrophys. **678**, A50 (2023).
[6] D. J. Reardon *et al.*, Astrophys. J. Lett. **951**, L6 (2023).
[7] H. Xu *et al.*, Res. Astron. Astrophys. **23**, 075024 (2023).
[8] S. Osłowski, W. van Straten, P. Demorest, and M. Bailes, Mon. Not. R. Astron. Soc. **430**, 416 (2013).
[9] T. Liu, X. Lou, and J. Ren, Phys. Rev. Lett. **130**, 121401 (2023).
[10] W. Hu, R. Barkana, and A. Gruzinov, Phys. Rev. Lett. **85**, 1158 (2000).
[11] L. Hui, J. P. Ostriker, S. Tremaine, and E. Witten, Phys. Rev. D **95**, 043541 (2017).
[12] D. H. Weinberg, J. S. Bullock, F. Governato, R. Kuzio de Naray, and A. H. Peter, Proc. Natl. Acad. Sci. U.S.A. **112**, 12249 (2015).
[13] E. G. M. Ferreira, Astron. Astrophys. Rev. **29**, 7 (2021).
[14] J. Zhang, J.-L. Kuo, H. Liu, Y.-L. S. Tsai, K. Cheung, and M.-C. Chu, Astrophys. J. **863**, 73 (2018).
[15] K. Hayashi, E. G. M. Ferreira, and H. Y. J. Chan, Astrophys. J. Lett. **912**, L3 (2021), #22102.05300.
[16] N. Dalal and A. Kravtsov, Phys. Rev. D **106**, 063517 (2022).
[17] L. Hui, Annu. Rev. Astron. Astrophys. **59**, 247 (2021).
[18] S. M. Carroll, G. B. Field, and R. Jackiw, Phys. Rev. D **41**, 1231 (1990).
[19] S. M. Carroll and G. B. Field, Phys. Rev. D **43**, 3789 (1991).
[20] A. Zic *et al.*, Publ. Astron. Soc. Aust. **40**, e049 (2023).
[21] S. D. M. White and M. J. Rees, Mon. Not. R. Astron. Soc. **183**, 341 (1978).
[22] J. W. Foster, N. L. Rodd, and B. R. Safdi, Phys. Rev. D **97**, 123006 (2018).
[23] G. P. Centers *et al.*, Nat. Commun. **12**, 7321 (2021).
[24] J. W. Foster, Y. Kahn, R. Nguyen, N. L. Rodd, and B. R. Safdi, Phys. Rev. D **103**, 076018 (2021).
[25] H. Nakatsuka, S. Morisaki, T. Fujita, J. Kume, Y. Michimura, K. Nagano, and I. Obata, Phys. Rev. D **108**, 092010 (2023).
[26] H.-Y. Schive, T. Chiueh, and T. Broadhurst, Nat. Phys. **10**, 496 (2014).
[27] One pulsar, J1824-2452, is located closer to the galactic center than the others in the PPPA, where the DM density is potentially higher. However, given the limited sensitivity of this pulsar to the ALDM signals, we do not anticipate a significant impact on the combined limits which are derived under the assumption of a uniform $\rho(\mathbf{x})$ for all PPPA pulsars.
[28] D. Harari and P. Sikivie, Phys. Lett. B **289**, 67 (1992).
[29] J. M. Weisberg, J. E. Everett, J. M. Cordes, J. J. Morgan, and D. G. Brisbin, Astrophys. J. **721**, 1044 (2010).
[30] W. Yan *et al.*, Astrophys. Space Sci. **335**, 485 (2011).
[31] H. M. Wahl *et al.* (NANOGrav Collaboration), Astrophys. J. **926**, 168 (2022); **941**, 210(E) (2022).
[32] T. Liu, G. Smoot, and Y. Zhao, Phys. Rev. D **101**, 063012 (2020).
[33] A. Caputo, L. Sberna, M. Frias, D. Blas, P. Pani, L. Shao, and W. Yan, Phys. Rev. D **100**, 063515 (2019).
[34] See Supplemental Material at http://link.aps.org/supplemental/10.1103/mptv-3x6g for additional calculations and explanations in support of the results presented in this Letter; includes Refs. [35–78].
[35] H. Xu, Y. X. Huang, M. Burgay, D. Champion, I. Cognard, L. Guillemot, J. Jang, R. Karuppusamy, M. Kramer, K. Lackeos *et al.*, Astronomer's Telegram **14642**, 1 (2021).
[36] J. Singha, M. P. Surnis, B. C. Joshi, P. Tarafdar, P. Rana, A. Susobhanan, R. Girgaonkar, N. Kolhe, N. Agarwal, S. Desai *et al.*, Mon. Not. R. Astron. Soc. **507**, L57 (2021).
[37] R. J. Jennings, J. M. Cordes, S. Chatterjee, M. A. McLaughlin, P. B. Demorest, Z. Arzoumanian, P. T. Baker, H. Blumer, P. R. Brook, T. Cohen *et al.*, Astrophys. J. **964**, 179 (2024).
[38] S. Johnston, D. Lorimer, P. Harrison, M. Bailes, A. Lynet, J. Bell, V. Kaspi, R. Manchester, N. D'Amico, L. Nleastrol *et al.*, Nature (London) **361**, 613 (1993).
[39] D. Reardon, G. Hobbs, W. Coles, Y. Levin, M. Keith, M. Bailes, N. Bhat, S. Burke-Spolaor, S. Dai, M. Kerr *et al.*, Mon. Not. R. Astron. Soc. **455**, 1751 (2016).
[40] J. Yao, R. Manchester, and N. Wang, Astrophys. J. **835**, 29 (2017).
[41] D. Lorimer, L. Nicastro, A. Lyne, M. Bailes, R. Manchester, S. Johnston, J. Bell, N. a. D'Amico, and P. Harrison, Astrophys. J. **439**, 933 (1995).
[42] D. J. Reardon, R. M. Shannon, A. D. Cameron, B. Goncharov, G. Hobbs, H. Middleton, M. Shamohammadi, N. Thyagarajan, M. Bailes, N. Bhat *et al.*, Mon. Not. R. Astron. Soc. **507**, 2137 (2021).
[43] S. Ransom, P. Ray, F. Camilo, M. Roberts, Ö. Çelik, M. Wolff, C. Cheung, M. Kerr, T. Pennucci, M. Decesar *et al.*, Astrophys. J. Lett. **727**, L16 (2010).
[44] M. Curyło *et al.*, Astrophys. J. **944**, 128 (2023).
[45] M. Bailes, S. Johnston, J. Bell, D. Lorimer, B. Stappers, R. Manchester, A. Lyne, L. Nicastro, N. d'Amico, and B. Gaensler, Astrophys. J. **481**, 386 (1997).
[46] M. Keith, S. Johnston, M. Bailes, S. Bates, N. Bhat, M. Burgay, S. Burke-Spolaor, N. D'Amico, A. Jameson, M. Kramer *et al.*, Mon. Not. R. Astron. Soc. **419**, 1752 (2012).
[47] F. Camilo, D. Nice, J. Shrauner, and J. Taylor, Astrophys. J. **469**, 819 (1996).
[48] M. Bailes, P. Harrison, D. Lorimer, S. Johnston, A. Lyne, R. Manchester, N. D'Amico, L. Nicastro, T. Tauris, and C. Robinson, Astrophys. J. **425**, L41 (1994).
[49] A. J. Faulkner, I. H. Stairs, M. Kramer, A. Lyne, G. Hobbs, A. Possenti, D. Lorimer, R. Manchester, M. McLaughlin, N. D'Amico *et al.*, Mon. Not. R. Astron. Soc. **355**, 147 (2004).
[50] M. Burgay, M. Bailes, S. Bates, N. Bhat, S. Burke-Spolaor, D. Champion, P. Coster, N. D'Amico, S. Johnston, M. Keith *et al.*, Mon. Not. R. Astron. Soc. **433**, 259 (2013).
[51] B. Jacoby, M. Bailes, S. Ord, H. Knight, and A. Hotan, Astrophys. J. **656**, 408 (2007).
[52] D. Lorimer, A. Lyne, M. Bailes, R. Manchester, N. D. Amico, B. Stappers, S. A. Johnston, and F. Camilo, Mon. Not. R. Astron. Soc. **283**, 1383 (1996).
[53] R. Foster, A. Wolszczan, and F. Camilo, Astrophys. J. **410**, L91 (1993).
[54] A. Lyne, A. Brinklow, J. Middleditch, S. Kulkarni, D. A. Backer, and T. Clifton, Nature (London) **328**, 399 (1987).
[55] D. Segelstein, L. Rawley, D. Stinebring, A. Fruchter, and J. Taylor, Nature (London) **322**, 714 (1986).

[56] B. A. Jacoby, M. Bailes, M. Van Kerkwijk, S. Ord, A. Hotan, S. Kulkarni, and S. Anderson, Astrophys. J. **599**, L99 (2003).
[57] D. C. Backer, S. R. Kulkarni, C. Heiles, M. Davis, and W. Goss, Nature (London) **300**, 615 (1982).
[58] M. Keith, S. Johnston, P. Ray, E. Ferrara, P. Saz Parkinson, Ö. Çelik, A. Belfiore, D. Donato, C. Cheung, A. Abdo *et al.*, Mon. Not. R. Astron. Soc. **414**, 1292 (2011).
[59] C. Sotomayor-Beltran, C. Sobey, J. W. T. Hessels, G. de Bruyn, A. Noutsos, A. Alexov, J. Anderson, A. Asgekar, I. M. Avruch, R. Beck *et al.*, Astron. Astrophys. **552**, A58 (2013).
[60] A. W. Hotan, W. van Straten, and R. N. Manchester, Publ. Astron. Soc. Aust. **21**, 302 (2004).
[61] J. E. Everett and J. M. Weisberg, Astrophys. J. **553**, 341 (2001).
[62] Z. Arzoumanian, P. T. Baker, L. Blecha, H. Blumer, A. Brazier, P. R. Brook, S. Burke-Spolaor, B. Bécsy, J. A. Casey-Clyde, M. Charisi *et al.*, Astrophys. J. Lett. **951**, L28 (2023).
[63] J. Yao, R. Manchester, and N. Wang, Astrophys. J. **835**, 29 (2017).
[64] J. L. Han, R. N. Manchester, A. G. Lyne, G. J. Qiao, and W. van Straten, Astrophys. J. **642**, 868 (2006).
[65] L. Lentati, P. Alexander, M. P. Hobson, F. Feroz, R. van Haasteren, K. J. Lee, and R. M. Shannon, Mon. Not. R. Astron. Soc. **437**, 3004 (2014).
[66] R. M. Shannon, S. Osłowski, S. Dai, M. Bailes, G. Hobbs, R. N. Manchester, W. van Straten, C. A. Raithel, V. Ravi, L. Toomey *et al.*, Mon. Not. R. Astron. Soc. **443**, 1463 (2014).
[67] G. M. Shaifullah, J. Magdalenic, C. Tiburzi, I. Jebaraj, E. Samara, and P. Zucca, Adv. Space Res. **72**, 5298 (2023).
[68] G. Agazie, A. Anumarlapudi, A. M. Archibald, Z. Arzoumanian, P. T. Baker, B. Bécsy, L. Blecha, A. Brazier, P. R. Brook, S. Burke-Spolaor *et al.*, Astrophys. J. Lett. **951**, L10 (2023).
[69] M. J. Keith, S. Johnston, A. Karastergiou, P. Weltevrede, M. E. Lower, A. Basu, B. Posselt, L. S. Oswald, A. Parthasarathy, A. D. Cameron *et al.*, Mon. Not. R. Astron. Soc. **530**, 1581 (2024).
[70] M. T. Lam, J. M. Cordes, S. Chatterjee, M. L. Jones, M. A. McLaughlin, and J. W. Armstrong, Astrophys. J. **821**, 66 (2016).
[71] J. Ellis and R. van Haasteren, JELLIS18/PTMCMCSampler: Official release, 10.5281/zenodo.1037579 (2017).
[72] P. M. Goggans and Y. Chi, AIP Conf. Proc. **707**, 59 (2004).
[73] B. Calderhead and M. Girolami, Computational Statistics and Data Analysis **53**, 4028 (2009).
[74] H. Kumamoto, S. Dai, S. Johnston, M. Kerr, R. M. Shannon, P. Weltevrede, C. Sobey, R. N. Manchester, G. Hobbs, and K. Takahashi, Mon. Not. R. Astron. Soc. **501**, 4490 (2021).
[75] M. J. Keith, W. Coles, R. M. Shannon, G. B. Hobbs, R. N. Manchester, M. Bailes, N. D. R. Bhat, S. Burke-Spolaor, D. J. Champion, A. Chaudhary *et al.*, Mon. Not. R. Astron. Soc. **429**, 2161 (2013).
[76] A. Derevianko, Phys. Rev. A **97**, 042506 (2018).
[77] B. P. Carlin and S. Chib, J. R. Stat. Soc. Ser. B **57**, 473 (1995).
[78] T. Lodewyckx, W. Kim, M. D. Lee, F. Tuerlinckx, P. Kuppens, and E.-J. Wagenmakers, J. Math. Psychol. **55**, 331 (2011).
[79] P. Salucci, F. Nesti, G. Gentile, and C. Frigerio Martins, Astron. Astrophys. **523**, A83 (2010).
[80] F. Nesti and P. Salucci, J. Cosmol. Astropart. Phys. 07 (2013) 016.
[81] G. Hobbs, R. N. Manchester, A. Dunning, A. Jameson, P. Roberts, D. George, J. A. Green, J. Tuthill, L. Toomey, J. F. Kaczmarek *et al.*, Publ. Astron. Soc. Aust. **37**, e012 (2020).
[82] R. N. Manchester, G. B. Hobbs, A. Teoh, and M. Hobbs, Astron. J. **129**, 1993 (2005).
[83] S. Dai *et al.*, Mon. Not. R. Astron. Soc. **449**, 3223 (2015).
[84] J. S. Hazboun, J. D. Romano, and T. L. Smith, Phys. Rev. D **100**, 104028 (2019).
[85] S. Adachi *et al.* (POLARBEAR Collaboration), Phys. Rev. D **110**, 063013 (2024).
[86] A. Castillo, J. Martin-Camalich, J. Terol-Calvo, D. Blas, A. Caputo, R. T. G. Santos, L. Sberna, M. Peel, and J. A. Rubiño Martín, J. Cosmol. Astropart. Phys. 06 (2022) 014.
[87] K. R. Ferguson *et al.* (SPT-3G Collaboration), Phys. Rev. D **106**, 042011 (2022).
[88] M. A. Fedderke, P. W. Graham, and S. Rajendran, Phys. Rev. D **100**, 015040 (2019).
[89] CAST Collaboration, Nat. Phys. **13**, 584 (2017).
[90] A. Payez, C. Evoli, T. Fischer, M. Giannotti, A. Mirizzi, and A. Ringwald, J. Cosmol. Astropart. Phys. 02 (2015) 006.
[91] J. S. Reynés, J. H. Matthews, C. S. Reynolds, H. R. Russell, R. N. Smith, and M. C. D. Marsh, Mon. Not. R. Astron. Soc. **510**, 1264 (2021).
[92] A. Khmelnitsky and V. Rubakov, J. Cosmol. Astropart. Phys. 02 (2014) 019.
[93] I. De Martino, T. Broadhurst, S. H. Henry Tye, T. Chiueh, H.-Y. Schive, and R. Lazkoz, Phys. Rev. Lett. **119**, 221103 (2017).
[94] N. K. Porayko *et al.*, Phys. Rev. D **98**, 102002 (2018).
[95] A. Afzal *et al.* (NANOGrav Collaboration), Astrophys. J. Lett. **951**, L11 (2023).
[96] C. Smarra *et al.* (European Pulsar Timing Array Collaboration), Phys. Rev. Lett. **131**, 171001 (2023).
[97] X. Li *et al.*, arXiv:2506.04871.
[98] M. Ajello *et al.* (Fermi-LAT Collaboration), Science **376**, abm3231 (2022).
[99] H. N. Luu, T. Liu, J. Ren, T. Broadhurst, R. Yang, J.-S. Wang, and Z. Xie, Astrophys. J. Lett. **963**, L46 (2024).
[100] Z.-Q. Xia, T.-P. Tang, X. Huang, Q. Yuan, and Y.-Z. Fan, Phys. Rev. D **107**, L121302 (2023).
[101] M. C. Weisskopf *et al.*, J. Astron. Telesc. Instrum. Syst. **8**, 026002 (2022).
[102] S.-N. Zhang *et al.* (eXTP Collaboration), Sci. China Phys. Mech. Astron. **62**, 29502 (2019).
[103] https://github.com/XueXiao-Physics/PPA.